https://doi.org/10.15407/ujpe65.5.369

O.V. BABAK,[1] YU.A. BEREZHNOY,[2] V.P. MIKHAILYUK[1]

[1] Institute for Nuclear Research, Nat. Acad. of Sci. of Ukraine
(47, Prosp. Nauky, Kyiv 03680, Ukraine; e-mail: avbabak@gmail.com)
[2] Karazin Kharkov National University
(4, Kharkov, Svobody Sq., 61077 Ukraine)

BORN APPROXIMATION FOR POLARIZATION OBSERVABLES AT THE SCATTERING OF PROTONS BY ^{40}Ca NUCLEI

A development of the optical model for the description of the hadron-nucleus scattering is proposed. When describing the behavior of polarization observables for the elastic proton scattering on ^{40}Ca nuclei in the energy interval from 200 to 800 MeV, the Born approximation is used. Analytical expressions for the scattering amplitudes, as well as for the differential cross-sections and polarization observables, are obtained. The comparison of the scattering observables calculated in the 1st and 2nd Born approximations is made. It is shown that the observables calculated in this approach are in a reasonable agreement with the available experimental data.

Keywords: optical model, Born approximation, intermediate energies, elastic scattering, polarization observables.

1. Introduction

The development of the optical model (see [1–6]) for investigations of the hadron scattering by nuclei is an important fundamental problem of nuclear physics.

In the optical model, the hadron-nucleus scattering is considered by analogy with the scattering of a wave of light by a liquid spherical drop, which is characterized by certain values of the refraction and absorption indices. The particle-nucleus scattering in this case is described by a complex potential, whose real part determines the scattered wave refraction in the nuclear matter, and its imaginary part characterizes the absorption of scattered particles by the nucleus.

The essence of the optical model lies in the fact that the multiparticle interaction of a projectile with individual nucleons of the nucleus or with other particles, which can exist in the nucleus, is replaced by an effective two-particle complex potential, i.e., the complicated multiparticle problem is reduced to a simple two-particle problem. This approach greatly simplifies the calculations of the scattering observables and finds good agreement with the experimental data, as well as with a number of more important fundamental physical arguments. Taking into account that the optical model is a powerful tool for explaining and interpreting a large number of experimental data in a wide range of energies, an important conclusion that the concept of nuclear matter is entirely realistic can be made. This matter is characterized by certain values of the refraction and absorption coefficients for each wavelength of a scattered hadron, i.e., its complex potential is equivalent to the complex refractive coefficient of the nuclear matter, and the imaginary part of such potential describes the absorption properties of the target nucleus. In this case, the absorption of incident particles should be considered as their

elimination from the elastic channel to various inelastic ones.

Accurate data for the elastic scattering of protons on ^{40}Ca and other nuclei are available in the bombarding energy interval from 200 to 800 MeV. Most of these data have been analyzed in terms of the standard optical model employing the real and imaginary parts of the potential in the Woods–Saxon form (see, e.g., [7–15]). Alternatively, the relativistic and nonrelativistic impulse approximations, as well as Dirac phenomenology for the description of such processes are used (see, e.g., [16–29]).

In such energy interval, the hadron-nucleus scattering amplitudes can also be considered in the Born approximation (BA) with the optical potential including the spin-orbit part which is, by analogy with the shell model, usually chosen in the Thomas form.

However, it turns out that the scattering amplitude calculated in the 1st BA with the Hermitian potential is real [30]. As a result, the polarization of the nucleons from nuclei is equal to zero in this approach. Therefore, when calculating the hadron-nucleus polarization observables, at least the 2nd BA should be used.

In the present work, we will obtain some analytical expressions for the amplitudes and polarization observables for the elastic scattering of protons on ^{40}Ca nuclei in the 1st and 2nd BA and make comparison between theoretical predictions and experimental data in the energy interval from 200 to 800 MeV.

In Sect. 2, we describe the theoretical formalism. Section 3 presents the results of calculations, and the comparison and discussion of the results are given in Sect. 4.

2. Theoretical Formalism

2.1. Scattering amplitudes and observables

The amplitude for the nucleon scattering on a zero-spin nucleus is a spin operator with the general structure

$$\hat{F}(\mathbf{k},\mathbf{k}') = F_c(\mathbf{k},\mathbf{k}') + F_s(\mathbf{k},\mathbf{k}')(\boldsymbol{\sigma}\mathbf{n}), \tag{1}$$

where $F_{c,s}(\mathbf{k},\mathbf{k}')$ are the central and spin-orbital amplitudes, $\boldsymbol{\sigma}$ is the spin operator of the incident nucleon, $\mathbf{n} = (\mathbf{k}\times\mathbf{k}')/|\mathbf{k}\times\mathbf{k}'|$, and $\mathbf{k}$, $\mathbf{k}'$ are the initial and final nucleon wave vectors.

The complete determination of the collision matrix $\hat{F}(\mathbf{k},\mathbf{k}')$ for the elastic proton scattering on zero-spin nuclei can be achieved by choosing a suitable set of independent observables. Usually, for this purpose, three independent observable as functions of the scattering angle are used [31]. A commonly used set of such observables includes the differential cross-section $\sigma(q) \equiv \mathrm{d}\sigma/\mathrm{d}\Omega$ and polarization (analyzing power) $\mathrm{P}(q)$, as well as one of the additional independent polarization observables, namely, the spin-rotation function $\mathrm{Q}(q)$. Unfortunately, due to an arbitrary scattering phase, the calculation of such observables does not allow one to determine unambiguously the amplitudes $F_i(\mathbf{k},\mathbf{k}')$. Therefore, the measurement and analysis of four suitably chosen observables are required [21].

The relations between such observables and the amplitudes $F_c(q)$ and $F_s(q)$ in (1) are

$$\sigma(q) = |F_c(q)|^2 + |F_s(q)|^2, \tag{2}$$

$$P(q)\sigma(q) = 2\mathrm{Re}\,(F_c(q)F_s^*(q)), \tag{3}$$

$$Q(q)\sigma(q) = 2\mathrm{Im}\,(F_c(q)F_s^*(q)), \tag{4}$$

$$S(q)\sigma(q) = |F_c(q)|^2 - |F_s(q)|^2, \tag{5}$$

$$\cos\beta(q) = \frac{S(q)}{\sqrt{Q^2(q)+S^2(q)}}, \tag{6}$$

where $\mathbf{q} = \mathbf{k} - \mathbf{k}'$, $|\mathbf{q}| = 2k\sin(\theta/2)$.

Note that, with regard for the available experimental data, we use the spin-rotation angle $\beta(q)$ as a fourth independent observable. This quantity can be interpreted [31] as the angle, by which the projection of the proton spin on the scattering plane rotates during the scattering.

In the Born approximation (BA), the scattering amplitudes $F_i(\mathbf{k},\mathbf{k}')$ $(i = c,s)$ are calculated under the assumption that the scattering field may be considered as a perturbation. In this assumption, the amplitude of the scattering of a particle in the nucleus can be presented as a series

$$F_i(\mathbf{k},\mathbf{k}') = \sum_{n=1}^{\infty} f^{(n)}(\mathbf{k},\mathbf{k}'), \tag{7}$$

where n is the perturbation power.

Retaining only the first two terms for the amplitudes $f^{(n)}(\mathbf{k},\mathbf{k}')$ in (7), we have

$$f^{(1)}(\mathbf{k},\mathbf{k}') = -\frac{m}{2\pi\hbar^2}\int d^3r e^{-i\mathbf{k}'\mathbf{r}}U(\mathbf{r})e^{i\mathbf{k}\mathbf{r}}, \tag{8}$$

$$f^{(2)}(\mathbf{k},\mathbf{k}') = -\frac{m}{2\pi\hbar^2}\int d^3r d^3r' e^{-i\mathbf{k}'\mathbf{r}} \times$$

$$\times U(\mathbf{r}')G_0^{(+)}(\mid \mathbf{r}-\mathbf{r}' \mid)U(\mathbf{r})e^{i\mathbf{k}\mathbf{r}}, \quad (9)$$

where $m = m_1m_2/(m_1+m_2)$ is the reduced mass of the colliding particles, and Green's function is determined by

$$G_0^{(+)}(\mid \mathbf{r}-\mathbf{r}' \mid) = -\frac{m}{2\pi\hbar^2}\frac{e^{ik|\mathbf{r}-\mathbf{r}'|}}{|\mathbf{r}-\mathbf{r}'|}. \quad (10)$$

2.2. Optical potential

The optical potential $U(\mathbf{r})$ with the spin-orbit part taken into account is

$$U(\mathbf{r}) = U_1(r) + U_2(r)(\boldsymbol{\sigma}\mathbf{l}). \quad (11)$$

In this formula, the radial parts of such potential were chosen in the form

$$U_1(r) = -V_0\{g_v(r) + i\varsigma g_w(r)\}, \quad (12)$$

$$U_2(r) = \lambda_\pi^2\frac{V_s(1+i\varsigma_s)}{r}\left\{\frac{dg_s(r)}{dr} + \gamma R_s\frac{d^2g_s(r)}{dr^2}\right\}. \quad (13)$$

Here, $\varsigma = W_0/V_0$, $\varsigma_s = W_s/V_s$, values V_j, W_j denote the strengths of the real, imaginary, and spin-orbit parts of the potential $U(\mathbf{r})$, respectively, the dimensionless parameter $\gamma = \Delta R/R$ determines a relative change of the radius of the real part of the optical potential $U(\mathbf{r})$ due to the allowance for the spin-orbit interaction, and $\lambda_\pi^2 = (\hbar/m_\pi c)^2 = 2$ fm^2 is the pion Compton wavelength factor traditionally used in similar calculations.

In (12) and (13), the values $g_j(r)$ are chosen in the Woods–Saxon form with regard for the differences between the parameters of the real, imaginary, and spin-orbit parts

$$g_j(r) = 1/\{1+\exp(r-R_j)/d_j)\}, \quad j = v,w,s. \quad (14)$$

When determining the form of the spin-orbit part of potential (11), the following arguments were used. Usually, the spin-orbit part of the potential $U(\mathbf{r})$ in the optical model is assumed to be real, and its radial shape is proportional to the density gradient. In this approach, the functional dependence of the potential $U_2(r)$ is close to the step function. But, for the parallel (+) and antiparallel (–) vectors $\mathbf{l}$ and $\boldsymbol{\sigma}$, this functional dependence has different radii and depths [32, 33].

Therefore, representing the spin-orbit part of the potential $U(\mathbf{r})$ as

$$U_2(r) \equiv U_2(r-R),\ U_2(r)^{(\pm)} = U_2(r-R\mp\frac{\gamma}{2}R),\ \gamma \ll 1, \quad (15)$$

and expanding the functions $U_2(r)^{(\pm)}$ into series, we have

$$U_2(r)^{(+)} - U_2(r)^{(-)} \approx -\gamma R\frac{dU_2(r)}{dr}, \quad (16)$$

which allows us to get the functional dependence (13).

Note that, in this approach, we do not consider the Coulomb interaction, because the contribution of this interaction is not very significant at the energy considered, whereas the theoretical calculations become noticeably complicated.

3. Calculations and Analysis

3.1. 1st Born approximation

Performing the integration in (8) and taking relations (11)–(14) into account, we get the scattering amplitude $f^{(1)}(\mathbf{k},\mathbf{k}')$ in the 1st BA as follows:

$$f^{(1)}(\mathbf{k},\mathbf{k}') = f_c(q) + f_s(q)(\boldsymbol{\sigma}\mathbf{n}), \quad (17)$$

$$f_c(q) = -\frac{2mV_0}{\hbar^2 q}\{R_vA_v(q) + i\varsigma R_wA_w(q)\}, \quad (18)$$

$$f_s(q) = -i\frac{2mR_sV_s}{\hbar^2 q}(1+i\varsigma_s)\lambda_\pi^2k^2\sin\theta \times$$

$$\times\{(1-\gamma)A_s(q) + \gamma B(q)\}. \quad (19)$$

Here, the amplitudes $A_j(q)$ and $B(q)$ read

$$A_j(q) = \frac{d}{dq}\tilde{A}_j(q),\ B(q) = \frac{d}{dq}\tilde{B}(q), \quad (20)$$

$$\tilde{A}_j(q) = F_{d_j}(q)j_0(qR_j),\ \tilde{B}(q) = qR_sF_{d_s}(q)j_1(qR_s). \quad (21)$$

In these formulae, $j_n(x)$ are the spherical Bessel functions, and the damping factor $F_{d_j}(q)$ has the form

$$F_{d_j}(q) = \frac{\pi\, qd_j}{\sinh(\pi\, qd_j)}, \quad j = v,w. \quad (22)$$

Using relations (2)–(6), we can calculate the complete set of observables for the elastic scattering of protons on ^{40}Ca nuclei in the energy interval from

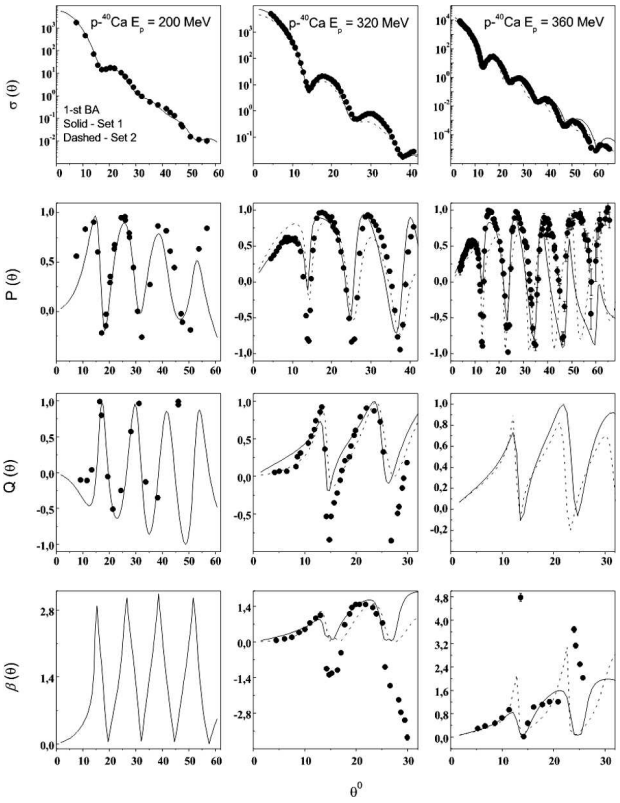

Fig. 1. Differential cross-section $\sigma(\theta) \equiv \mathrm{d}\sigma/\mathrm{d}\Omega$ (mb/sr), polarization $\mathrm{P}(\theta)$, spin-rotation function $\mathrm{Q}(\theta)$, and spin-rotation angle $\beta(\theta)$ for the 200, 320, and 360 MeV proton elastic scatterings on ^{40}Ca nuclei. The experimental data are taken from [10–12, 21]. The description of the curves is given in the text

Table 1. **Parameters of the optical potential obtained in the first Born approximation. Set 1**

E, MeV	V_0, MeV	W_0, MeV	d_V, fm	R_V, fm	d_W, fm	R_W, fm	V_s, MeV	W_s, MeV	d_s, fm	R_s, fm	γ
200	11.39	4.55	0.53	4.96	0.30	3.95	1.22	-0.80	0.82	4.94	0.29
320	16.51	9.35	0.55	4.46	0.43	3.90	–1.10	–1.44	0.70	3.47	-0.30
360	17.98	12.82	0.55	4.45	0.46	3.89	–0.09	–1.32	0.67	3.45	–0.28
500	20.75	14.03	0.56	4.50	0.46	3.89	–0.09	–1.30	0.66	3.43	–0.28
650	27.38	15.92	0.57	4.42	0.46	3.91	–0.05	–0.84	0.65	3.42	–0.28
800	37.72	19.31	0.58	4.31	0.49	4.03	–0.02	–0.57	0.61	3.39	–0.27

200 to 800 MeV. The results of such calculations in the 1st BA are given in Figs. 1 and 2.

We have obtained two alternative sets of the optical potential parameters both for the 1st BA (see Tables 1 and 2) and the 2nd BA (see Tables 3 and 4 below). The results are presented in all Figures by solid (for Set 1) and dashed (for Set 2) curves, respectively. As is seen from Figs. 1 and 2, the theoretical calculations performed in the 1st BA are in reasonable agreement with the available experimental data.

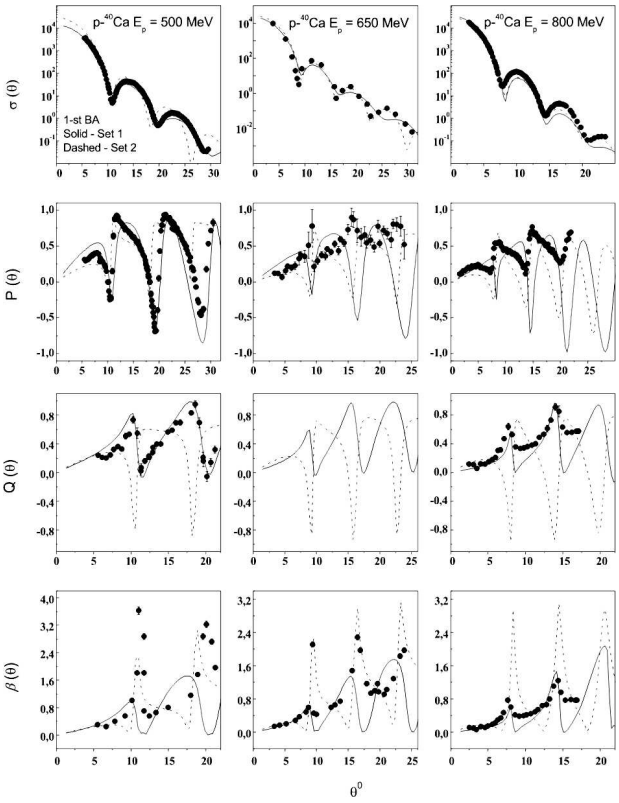

Fig. 2. The same as in Fig. 1, but for the 500, 650, and 800 MeV proton energies. The experimental data are taken from [16–21]

Table 2. **Parameters of the optical potential obtained in the first Born approximation. Set 2**

E, MeV	V_0, MeV	W_0, MeV	d_V, fm	R_V, fm	d_W, fm	R_W, fm	V_s, MeV	W_s, MeV	d_s, fm	R_s, fm	γ
320	9.70	–10.75	0.39	4.07	0.51	4.63	–1.44	–0.72	0.82	3.25	–0.29
360	2.50	–24.63	0.38	3.51	0.55	4.45	–1.13	0.85	0.64	3.91	–0.03
500	2.49	–36.27	0.37	3.37	0.55	4.36	–0.63	0.66	0.65	3.90	–0.33
650	2.29	–37.71	0.37	3.25	0.55	4.24	–0.28	0.45	0.66	3.90	–0.39
800	1.92	–41.01	0.31	3.11	0.51	4.22	–0.19	0.32	0.68	4.12	–0.43

Unfortunately, the approach using 1st BA is not entirely correct. This statement can be verified by calculating the observables in (2)–(5).

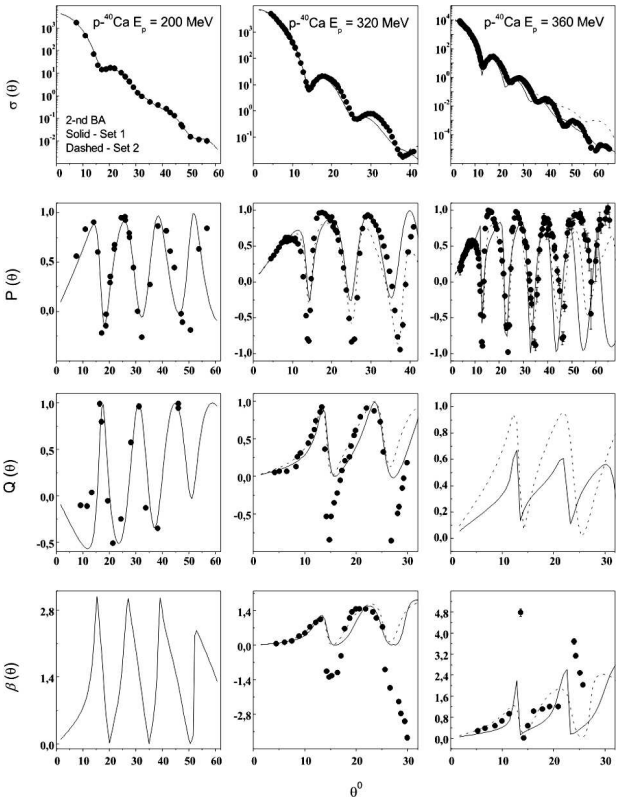

Fig. 3. The same as in Fig. 1, but for 2nd BA

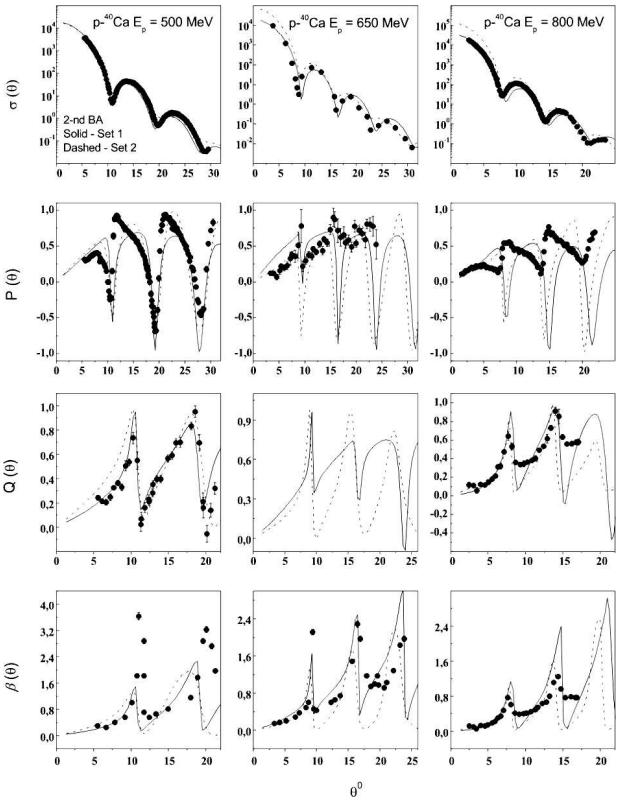

Fig. 4. The same as in Fig. 2, but for 2nd BA

Using relations (17)–(22) and assuming, for simplicity, $R_v = R_w = R_s \equiv R, d_v = d_w = d_s \equiv d$ in (18) and (19), the analytical expressions for such observables in the 1st BA can be presented as

$$\sigma(q) = R^2 \left(\frac{2mV_0}{\hbar^2 q}\right)^2 \sigma_1(q), \tag{23}$$

$$\sigma_1(q) = \left(1+\varsigma^2\right) A^2(q) +$$

$$+ \lambda_\pi^4 k^4 \sin^2\theta \left\{(1-\gamma)\, A(q) + \gamma B(q)\right\}^2, \tag{24}$$

$$P(q)\sigma_1(q) = \varsigma 2\lambda_\pi^2 k^2 \sin\theta A(q) \times$$

$$\times \left\{(1-\gamma)\, A(q) + \gamma B(q)\right\}, \tag{25}$$

$$Q(q)\sigma_1(q) = -2\lambda_\pi^2 k^2 \sin\theta A(q) \times$$

$$\times \left\{(1-\gamma)\, A(q) + \gamma B(q)\right\}, \tag{26}$$

$$S(q)\sigma_1(q) = \left(1+\varsigma^2\right) A^2(q) -$$

$$- \lambda_\pi^4 k^4 \sin^2\theta \left\{(1-\gamma)\, A(q) + \gamma B(q)\right\}^2. \tag{27}$$

As can be seen from the above formulae, the polarization calculated in the 1st BA with the Hermitian potential ($\varsigma = 0$) is equal to zero. Therefore, when calculating the polarization observables for the scattering of particles on nuclei with the use of BA, at least the 2nd BA should be applied.

3.2. 2nd Born approximation

In the 2nd BA, the amplitude $f^{(2)}(\mathbf{k}, \mathbf{k}')$ is determined by Eq. (9). When calculating the integral in (9), we used the approximation $d/R \ll 1$, as well as the expansion of the potentials $U_i(r)$ $(i = 1, 2)$ in series up to the first significant terms

$$U(|\mathbf{u} + \mathbf{r}'|) \simeq U(u) + \frac{\mathbf{u}\mathbf{r}'}{u} \frac{dU(u)}{du}, \tag{28}$$

where $|\mathbf{u} + \mathbf{r}'| \simeq u + \mathbf{u}\mathbf{r}'/u, \quad \mathbf{u} = \mathbf{r} - \mathbf{r}'$.

This expansion can be justified by the fact that Green's function $G_0^{(+)}(|\ \mathbf{r} - \mathbf{r}'\ |)$ in (10) has a maximum at $|\mathbf{r}| \approx |\mathbf{r}|'$.

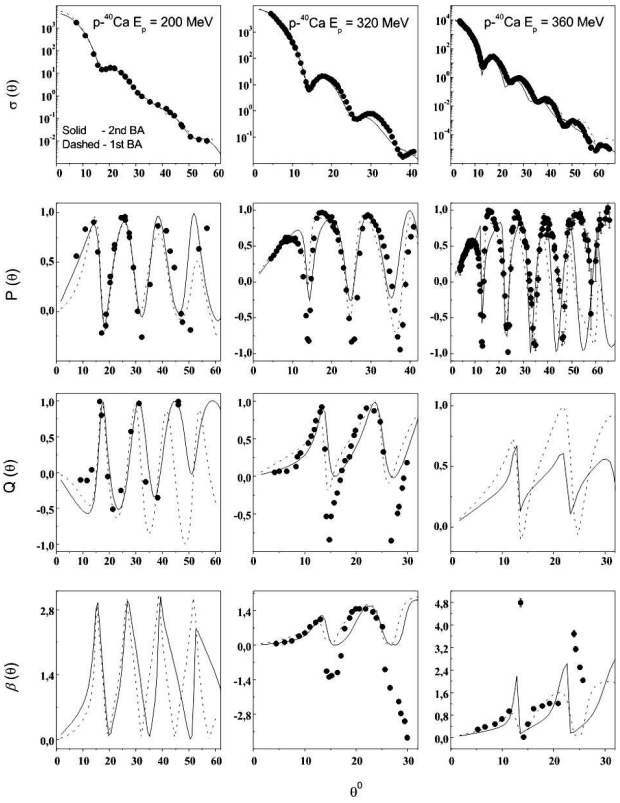

Fig. 5. Comparison of the observables obtained within the 2nd and 1st BA for the 200, 320, and 360 MeV proton elastic scatterings on ^{40}Ca nuclei. The experimental data are taken from [10–12, 21]. For the description of the curves, see the text

Performing the integration in (9) and taking relations (11)–(14) and (28) into account, we obtain the scattering amplitude $f^{(2)}(\mathbf{k},\mathbf{k}')$:

$$f^{(2)}(\mathbf{q}) = f_{cc}(q) + f_{ss}(q) + 2f_{cs}(q)(\boldsymbol{\sigma}\mathbf{n}), \quad (29)$$

$$f_{cc}(q) = \frac{mV_0}{2k^2\hbar^2}\left\{\mathcal{F}_1^{(l)}(k)f_c(q) + q\mathcal{F}_2^{(l)}(k)\frac{df_c(q)}{dq}\right\}, \quad (30)$$

$$\mathcal{F}_j^{(l)}(k) = \mathcal{F}_j^{(v)}(k) + i\varsigma\mathcal{F}_j^{(w)}(k), \quad j = 1,2, \quad (31)$$

$$\mathcal{F}_1^{(l)}(k) = 1 + 2ikR_l - e^{2ikR_l}F_{d_l}(2k), \quad (32)$$

$$\mathcal{F}_2^{(l)}(k) = 1 + e^{2ikR_l}F_{d_l}(2k) - 2j_0(kR_l)\,e^{ikR_l},\ l = v,w, \quad (33)$$

$$f_{ss}(q) =$$
$$= kR_s\cos^2\theta\left(\frac{4mV_s}{\hbar^2}(1+i\varsigma_s)\right)^2\left\{k\frac{d}{dk'} - \frac{d}{dk'}k'\right\}\times$$
$$\times\frac{d}{dk}\left[\left\{(1-\gamma)\tilde{A}_s(q) + \gamma\tilde{B}(q)\right\}\left(1-\gamma R_s\frac{d}{dR_s}\right)\times\right.$$
$$\times j_0(k'R_s)\,e^{ikR_s} - \frac{k\cos\theta - k'}{q}\frac{d}{dk'}\times$$
$$\times\{(1-\gamma)A_s(q) + \gamma B(q)\}\times$$
$$\left.\times\frac{d}{dR_s}\left(1-\gamma R_s\frac{d}{dR_s}\right)\frac{1}{R_s}j_0(k'R_s)\left(e^{ikR_s}-1\right)\right], \quad (34)$$

where the amplitudes $f_{c,s}(q)$ are determined by Eqs. (18) and (19).

Note that the form of the amplitude $f_{cs}(q)$ in (29) is the same as that given in (30)–(33), where the amplitude $f_c(q)$ (18) should be replaced by $f_s(q)$ (19).

Finally, for the amplitudes $F_i(\mathbf{k},\mathbf{k}')$ (1) in the 2nd BA, we have

$$F_c(q) = f_c(q) + f_{cc}(q) + f_{ss}(q),\ F_s(q) = f_s(q) + 2f_{cs}(q). \quad (35)$$

The results of calculations within such approach are presented in Figs. 3 and 4, and the parameters of the optical potential are given in Tables 3 and 4.

As is seen from Figs. 3 and 4, the results of calculations performed in the 2nd BA are in reasonable agreement with the available experimental data for both sets of the parameters used.

Table 3. **Parameters of the optical potential obtained in the 2nd Born approximation. Set 1**

E, MeV	V_0, MeV	W_0, MeV	d_V, fm	R_V, fm	d_W, fm	R_W, fm	V_s, MeV	W_s, MeV	d_s, fm	R_s, fm	γ
200	12.81	13.35	0.51	4.79	0.53	4.46	1.89	–1.67	0.72	4.31	0.13
320	19.87	16.33	0.52	4.44	0.53	3.79	–0.40	–1.39	0.69	4.39	0.12
360	21.57	20.13	0.56	4.33	0.53	4.28	–0.52	–1.13	0.65	3.65	–0.11
500	29.06	25.75	0.66	4.32	0.49	4.22	–0.50	–1.01	0.61	3.61	–0.14
650	31.06	35.75	0.72	4.10	0.43	4.21	–0.40	–1.17	0.58	3.60	–0.17
800	40.34	45.53	0.76	4.34	0.40	4.12	–0.21	–0.70	0.46	3.60	–0.07

Table 4. **Parameters of the optical potential obtained in the 2nd Born approximation. Set 2**

E, MeV	V_0, MeV	W_0, MeV	d_V, fm	R_V, fm	d_W, fm	R_W, fm	V_s, MeV	W_s, MeV	d_s, fm	R_s, fm	γ
320	9.89	–9.62	0.41	4.10	0.54	4.66	–0.89	–0.19	0.60	3.56	–0.15
360	4.78	–14.64	0.26	3.45	0.58	4.31	–0.80	0.54	0.59	3.56	–0.13
500	4.74	–19.83	0.24	3.37	0.60	4.29	–0.78	0.49	0.58	3.59	–0.17
650	4.35	–35.68	0.22	3.34	0.60	4.35	–0.58	0.35	0.61	3.70	–0.13
800	4.21	–46.30	0.21	3.20	0.59	4.36	–0.52	0.35	0.62	3.81	–0.05

4. Discussion

In Figs. 5 and 6, we present the comparison of the results obtained with the use of the 2nd and 1st BA. In these figures, the solid and dashed curves were calculated in the 2nd and 1st BA, respectively, using the parameters of the optical potential from Tables 1 and 3 (Set 1).

As Figs. 5 and 6 show, the 2nd BA allows us to describe the available experimental data more precisely as compared with the 1st BA.

Note that, despite the rather good agreement between the calculated and measured observables, the parameters of the optical potential cannot be determined quite reliably for the energies 200, 360, and 650 MeV due to the lack of a complete set of measured independent observables.

As was mentioned above, two alternative sets of the optical potential parameters both for the 1st and 2nd BA (see Tables 1–4) were obtained. Using these

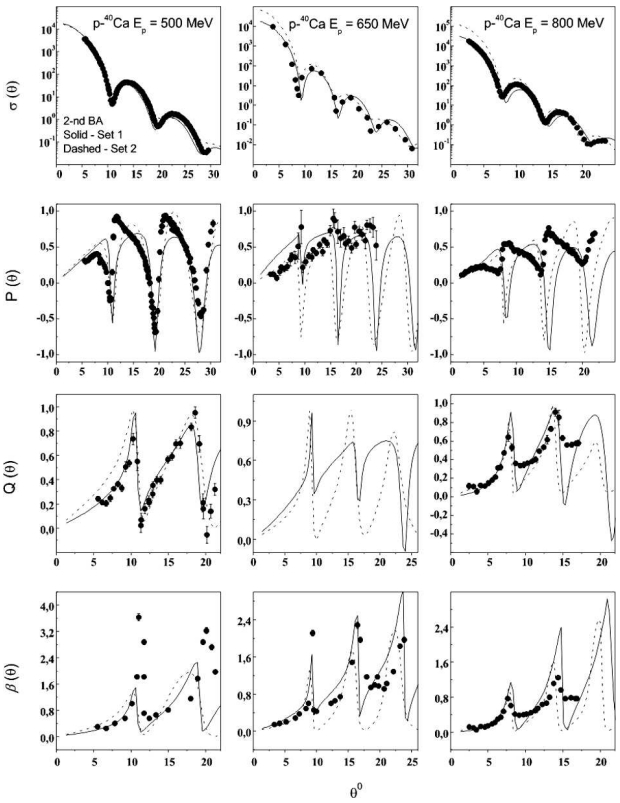

Fig. 6. The same as in Fig. 5, but for the 500, 650, and 800 MeV proton energies. The experimental data are taken from [16–21]

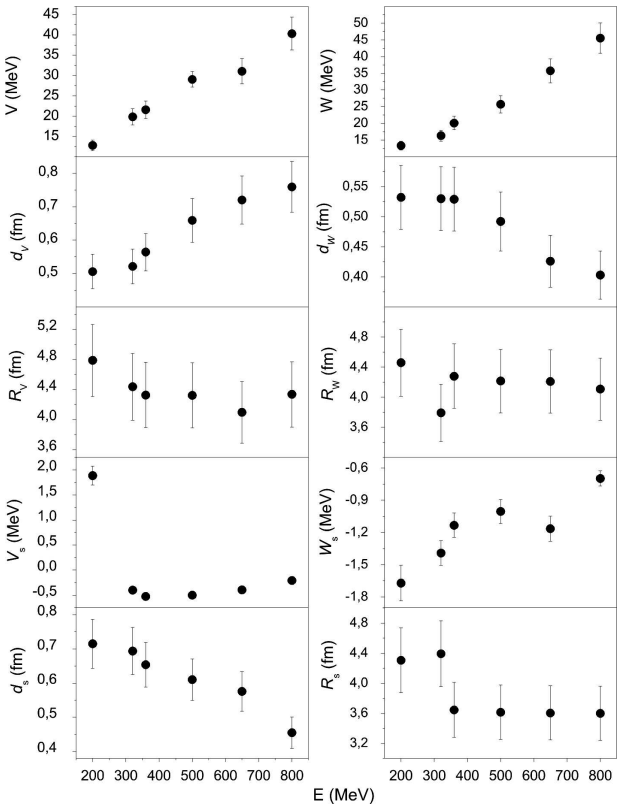

Fig. 7. Energy dependence of the optical potential parameters in the 2nd BA

sets of parameters, we have calculated the scattering observables shown in Figs. 1–6.

As an example, the energy dependence of the parameters obtained in the 2nd BA (see Table 3) is presented in Fig. 7.

As is seen from Tables 1–4 and Fig. 7, the energy dependence of the optical potential parameters is sufficiently smooth. The only exceptions are the parameters at the 200 MeV energy. This can be explained by the transition from the diffraction scattering conditions at higher energies to the scattering with essential refractive effects at lower energies [34].

In addition, we are dealing with the well-known problem of discrete ambiguities in the values of the optical potential parameters. This problem was considered in detail for composite incident particles at a lower energies (see, e.g., [35, 36]). But, for the proton-nucleus scattering at intermediate energies, such problem was not considered yet thoroughly and requires a further study.

Note that, for energies up to 180 MeV, the empirical relations for the energy dependence of the optical potential parameters have been obtained (see, e.g., [7–9]). Obviously, the parameters of the optical potential obtained in the BA approach should not be the same as those obtaining from the numerical solution of the Schrödinger equation. At the same time, the obtained values of such parameters must not differ significantly from those obtained in other similar calculations. As Tables 1 and 3 show, for the 200 MeV energy, the values of such parameters in the BA approach coincide with those, presented in [7–9].

5. Summary and Conclusions

The investigation of the interaction of intermediate-energy particles with nuclei attracts a great interest during many decades of the development of nuclear physics. This interest is motivated by the possibility of studying the basic properties and structure of the colliding nuclei and the mechanism of their interaction.

Various approaches were used to study such processes. For example, the multiple proton scattering on nuclei was considered, by including "elementary" nucleon–nucleon amplitudes [37], and various microscopic optical potentials were discussed in [38]. In [34], we introduced the approach based on the α-cluster model with dispersion, which allowed us to describe a large amount of the experimental data for the elastic and inelastic scattering of protons in light nuclei from ^{9}Be to ^{24}Mg.

Here, we have used the 2nd BA to study the proton-nucleus scattering at intermediate energies, because the scattering amplitude calculated in the 1st BA with the Hermitian potential is real, and the polarization of the nucleons from nuclei is equal to zero. Therefore, when calculating the hadron-nucleus polarization observables, at least the 2nd BA should be used.

The analytical expressions for the amplitudes and observables for the elastic scattering of protons on ^{40}Ca nuclei in the 1st and 2nd BA are obtained, and the comparison between theoretical predictions and experimental data in the energy interval from 200 to 800 MeV is given.

The results show that the calculations performed in the 2nd BA give possibility to describe the available experimental data quite well and more precisely, as compared with those obtained in the 1st BA.

1. H. Feshbach, C.E. Porter, V.F. Weisskopf. The formation of a compound nucleus in neutron reactions. *Phys. Rev.* **90**, 166 (1953).
2. H. Feshbach, C.E. Porter, V.F. Weisskopf. Model for nuclear reactions with neutrons. *Phys. Rev.* **96**, 448 (1954).
3. H. Feshbach. Unified theory of nuclear reactions. *Ann. Phys.* **5**, 357 (1958).
4. P.E. Hodgson, *Nuclear Reactions and Nuclear Structure*, (Clarendon Press, 1971). [ISBN-10: 0198512619].
5. H. Feshbach. A unified theory of nuclear reactions. *Ann. Phys.* (New York) **281**, 519 (2000).
6. R.D. Woods, D.S. Saxon. Diffuse surface optical model for nucleon-nuclei scattering. *Phys. Rev.* **95**, 577 (1954).
7. W.T.H. van Oers. Optical-model analysis of p+^{40}Ca elastic scattering from 10–180 MeV *Phys. Rev. C* **3**, 1550 (1971).
8. A. Nadasen, P. Schwandt, P.P. Singh, W.W. Jacobs, A.D. Bacher, P.T. Debevec, M.D.Kaitchuck, J.T. Meek. Elastic scattering of 80–180 MeV protons and the proton-nucleus optical potential. *Phys. Rev. C* **23**, 1023 (1981).
9. P. Schwandt, H.O. Meyer, W.W. Jacobs, A.D. Bacher, S.E. Vigdor, M.D. Kaitchuck, T.R. Donoghue. Analyzing power of proton-nucleus elastic scattering between 80 and 180 MeV. *Phys. Rev. C* **26**, 55 (1982).
10. H. Seifert, J.J. Kelly, A.E. Feldman, B.S. Flanders, M.A. Khandaker, Q. Chen, A.D. Bacher, G.P.A. Berg, E.J. Stephenson, P. Karen, B.E. Norum, P. Welch, A. Scott. Effective interaction for ^{16}O(p,p') and ^{40}Ca(p,p') at $E_p = 200$ MeV. *Phys. Rev. C* **47**, 1615 (1993).
11. J.J. Kelly, P. Boberg, A.E. Feldman, B.S. Flanders, M.A. Khandaker, S.D. Hyman, H. Seifert, P. Karen, B.E. Norum, P. Welch, S. Nanda, A. Saha. Effective interaction for ^{40}Ca(p,p') at $E_p = 318$ MeV. *Phys. Rev. C* **44**, 2602 (1991).
12. D. Frekers, S.S.M. Wong, R.E. Azuma, T.E. Drake, J.D. King, R. Abegg, K.P. Jackson, C.A. Miller, S. Yen, W.P. Alford, R.L. Helmer, C. Broude, S. Mattsson, E. Rost. Elastic and inelastic scattering of 362 MeV polarized protons from ^{40}Ca *Phys. Rev. C* **35**, 2236 (1987).
13. D.A. Hutcheon, W.C. Olsen, H.S. Sherif, R. Dymarz, J.M. Cameron, J. Johansson, P. Kitching, P.R. Liljestrand, W.J. McDonald, C.A. Miller, G.C. Neilson, D.M. Sheppard, D.K. McDaniels, J.R. Tinsley, P. Schwandt, L.W. Swenson, C.E. Stronach. The elastic scattering of intermediate energy protons from ^{40}Ca and ^{208}Pb. *Nucl. Phys. A* **483**, 1 (1988).
14. A. Nadasen, S. Balaji, J. Brace, K.A.G. Rao, P.G. Roos, P. Schwandt, J.T. Ndefru. Nucleon elastic scattering potentials: Energy and isospin dependence. *Phys. Rev. C* **66**, 064605 (2002).
15. A.J. Koning, J.P. Delaroche. Local and global nucleon optical models from 1 keV to 200 MeV. *Nucl. Phys. A* **713**, 213 (2003).
16. G. Igo, G.S. Adams, T.S. Bauer, G. Pauletta, C.A. Whitten, Jr., A. Wriekat, G.W. Hoffmann, G.S. Blanpied, W.R. Coker, C. Harvey, R.P. Liljestrand, L. Ray, J.E. Spencer, H.A. Thiessen, C. Glashausser, N.M. Hintz,

M.A. Oothoudt, H. Nann, K.K. Seth, B.E. Wood, D.K. McDaniels, M. Gazzaly. Elastic differential cross-sections and analyzing powers for p+^{40,42,44,48}Ca at 0.8 GeV. *Phys. Lett. B* **81**, 151 (1979).
17. L. Ray, G.W. Hoffmann, M. Barlett, J. McGill, J. Amann, G. Adams, G. Pauletta, M. Gazzaly, G.S. Blanpied. Proton elastic scattering from ^{40,42,44,48}Ca at 800 MeV. *Phys. Rev. C* **23**, 828 (1981).
18. R.W. Fergerson, M.L. Barlett, G.W. Hoffmann, J.A. Marshall, E.C. Milner, G. Pauletta, L. Ray, J.F. Amann, K.W. Jones, J.B. McClelland, M. Gazzaly, G.J. Igo. Spin-rotation parameter Q for 800 MeV proton elastic scattering from ^{16O,40}Ca, and ^{208}Pb *Phys. Rev. C* **33**, 239 (1986).
19. B. Aas, E. Bleszynski, M. Bleszynski, M. Hajisaeid, G.J. Igo, F. Irom, G. Pauletta, A. Rahbar, A.T.M. Wang, C.F. Amann, T.A. Carey, W.D. Cornelius, J.B. McClelland, M. Barlett, G.W. Hoffmann, M. Gazzaly. Proton polarization observables for the elastic and inelastic scattering of 500 MeV protons from ^{40}Ca and ^{208}Pb. *Nucl. Phys. A* **446**, 675 (1986).
20. G.W. Hoffmann, M.L. Barlett, G. Pauletta, L. Ray, J.F. Amann, K. Ones, J.B. McClelland, R.W. Fergerson, M.M. Gazzaly, B.C. Clark, R.L. Mercer. Large angle p+^{40}Ca elastic scattering at 497.5 MeV. *Phys. Rev. C* **37**, 1307 (1988).
21. E. Bleszynski, B. Aas, D. Adams, M. Bleszynski, G.J. Igo, T. Jaroszewicz, A. Ling, D. Lopiano, F. Sperisen, M.G. Moshi, C.A. Whitten, Jr., C.A. Whitten, K. Jones, J.B. McClelland. Energy dependence of relativistic effects in the elastic scattering of polarized protons from ^{16}O and ^{40}Ca. *Phys. Rev. C* **37**, 1527 (1988).
22. L.G. Arnold, B.C. Clark, E.D. Cooper, H.S. Sherif, D.A. Hutcheon, P. Kitching, J.M. Cameron, R.P. Liljestrand, R.N. MacDonald, W.J. McDonald, C.A. Miller, G.C. Neilson, W.C. Olsen, D.M. Sheppard, G.M. Stinson, D.K. McDaniels, J.R. Tinsley, R.L. Mercer, L.W. Swenson, P. Schwandt, C.E. Stronach. Energy dependence of the p-^{40}Ca optical potential: A Dirac equation perspective. *Phys. Rev. C* **25**, 936 (1982).
23. J.A. McNeil, L. Ray, S.J. Wallace. Impulse approximation NN amplitudes for proton-nucleus interactions. *Phys. Rev. C* **27**, 2123 (1983).
24. B.C. Clark, S. Hama, R.L. Mercer, L. Ray, G.W. Hoffmann, B.D. Serot. Dirac-equation impulse approximation for intermediate-energy nucleon-nucleus scattering. *Phys. Rev. Lett.* **50**, 1644 (1983).
25. N. Ottenstein, S.J. Wallace, J.A. Tjon. Elastic scattering of protons by ^{16}O, ^{40}Ca, and ^{208}Pb at 200, 500, and 800 MeV: Relativistic and nonrelativistic analyses based on the impulse approximation. *Phys. Rev. C* **38**, 2272 (1988).
26. N. Ottenstein, S.J. Wallace, J.A. Tjon.Elastic scattering of protons by ^{16}O, ^{40}Ca, and ^{208}Pb at 200, 500, and 800 MeV: Effects of vacuum polarization and Pauli-blocking corrections. *Phys. Rev. C* **38**, 2289 (1988).
27. S. Hama, B.C. Clark, E.D. Cooper, H.S. Sherif, R.L. Mercer. Global Dirac optical potentials for elastic proton scattering from heavy nuclei. *Phys. Rev. C* **41**, 2737 (1990).
28. R.D. Amado, J. Piekarewicz, D.A. Sparrow, J.A. McNeil. Intermediate-energy-proton scattering, the Dirac equation, and nuclear structure. *Phys. Rev. C* **28**, 2180 (1983).
29. J.J. Kelly, S.J. Wallace. Comparison between relativistic and nonrelativistic models of the nucleon-nucleon effective interaction. I. Normal-parity isoscalar transitions. *Phys. Rev. C* **49**, 1315 (1994).
30. Yu.A. Berezhnoy, V.P. Mikhailyuk. Polarization of protons in the optical model. *Chinese Phys. C* **41**, 024102 (2017).
31. L. Wolfenstein. Polarization of fast nucleons. *Annu. Rev. Nucl. Sci.* **6**, 43 (1956).
32. A. Dar, B. Kozlowsky. Polarization in meson-baryon elastic scattering at high energies. *Phys. Lett.* **20**, 314 (1966).
33. S. Varma. Polarization in elastic scattering at low energies. *Nucl. Phys. A* **97**, 282 (1967).
34. Yu.A. Berezhnoy, V.P. Mikhailyuk, V.V. Pilipenko. Intermediate energy multiple scattering of particles by light α-cluster nuclei. *Int. J. Mod. Phys. E* **24**, 1530004 (2015).
35. D.A. Goldberg, S.M. Smith. Criteria for the elimination of discrete ambiguities in nuclear optical potentials. *Phys. Rev. Lett.* **29**, 500 (1972).
36. D.A. Goldberg, S.M. Smith, H.G. Pugh, P.Q. Boos, N.S. Wall. Scattering of 139-MeV alpha particles by ^{58}Ni and ^{208}Pb. *Phys. Rev.* **7**, 1938 (1973).
37. G.D. Alkhazov, S.L. Belostotsky, A.A. Vorobyov. Scattering of 1 GeV protons on nuclei. *Phys. Rep.* **42**, 89 (1978).
38. L. Ray, G.W. Hoffmann, W.R. Coker. Nonrelativistic and relativistic descriptions of proton-nucleus scattering. *Phys. Rep.* **212**, 223 (1992).

Received 22.08.19

О.В. Бабак, Ю.А. Бережной, В.П. Михайлюк

БОРНОВЕ НАБЛИЖЕННЯ
ДЛЯ ПОЛЯРИЗАЦІЙНИХ СПОСТЕРЕЖУВАНИХ
ПРИ РОЗСІЯННІ ПРОТОНІВ ЯДРАМИ ^{40}Ca.

Р е з ю м е

Запропоновано розвиток оптичної моделі для опису адрон-ядерного розсіяння. Для опису поляризаційних характеристик пружного розсіяння протонів ядрами ^{40}Ca в діапазоні енергій від 200 до 800 МеВ використовувалось борнове наближення. Отримано аналітичні вирази для амплітуд розсіяння, диференціальних перерізів та поляризаційних характеристик. Виконано порівняння спостережуваних характеристик розсіяння, розрахованих у 1-му та 2-му борновому наближенні. Доведено, що розраховані в цьому підході спостережувані характеристики добре узгоджуються з наявними експериментальними даними.